

Dielectric functions of densely stacked Si nanocrystal layer embedded in SiO₂ thin films

L. Ding,^{a)} T. P. Chen,^{b)} J. I. Wong, M. Yang, Y. Liu, and C. Y. Ng
*School of Electrical and Electronic Engineering, Nanyang Technological University,
 Singapore 639798, Singapore*

Y. C. Liu
Singapore Institute of Manufacturing Technology, Singapore 638075, Singapore

C. H. Tung and A. D. Trigg
Institute of Microelectronics, Singapore 117685, Singapore

S. Fung
Department of Physics, The University of Hong Kong, Hong Kong

(Received 3 October 2006; accepted 13 November 2006; published online 21 December 2006)

A densely stacked silicon nanocrystal layer embedded in a SiO₂ thin film is synthesized with Si ion implantation. The dielectric functions of the nanocrystal layer are determined with spectroscopic ellipsometry. The dielectric functions show a significant suppression as compared to that of bulk crystalline Si. Thermal annealing leads to an evolution of the dielectric functions from the amorphous towards crystalline state. For an insufficient annealing, the dielectric functions present a single broad peak, being similar to that of amorphous Si. However, a sufficient annealing leads to the emergence of the two-peak structure which is similar to that of bulk crystalline Si. In addition, the dielectric functions increase with annealing with a trend towards bulk Si. © 2006 American Institute of Physics. [DOI: 10.1063/1.2410227]

Over the past decade, there has been increasing research interest in the low dimensional silicon materials due to their potential applications in the optoelectronic devices, nonvolatile memory devices, and single electron devices. One promising approach of forming such low dimensional silicon is Si⁺ implantation into SiO₂ thin films. With this technique, isolated Si nanocrystals (nc-Si) dispersedly distributed in a SiO₂ matrix^{1–5} or densely stacked silicon nanocrystal layers embedded in SiO₂ (Refs. 6–9) can be formed depending on the implantation recipe. The former could be used for Si optoelectronic applications^{10,11} while the latter could be used in memory devices.^{7,9}

There have been both experimental^{3,4} and theoretical^{12,13} studies on the optical properties of isolated nc-Si dispersedly distributed in dielectrics. The optical properties of continuous thin film of nc-Si synthesized by pulsed laser pyrolysis of silane have been determined with spectroscopic ellipsometry also.¹⁴ However, no studies on the optical properties of the densely stacked Si nanocrystal layer synthesized by ion implantation have been reported so far. The optical properties of the densely stacked nanocrystal layer should be different from that of both the isolated nc-Si and the continuous nc-Si film. It is necessary to investigate the optical properties of the densely stacked nanocrystal layer because of the importance of such nanoscale structure in both fundamental physics and applications. In practice, the Si ion implantation into a thin SiO₂ film with a high dose (typically in the range of $\sim 10^{16}$ – $\sim 10^{17}$ cm⁻²) at a very-low energy (≤ 2 keV) can form such densely stacked nanocrystal layers embedded in SiO₂.^{6–9} In this work, the dielectric functions of the densely stacked Si nanocrystal layer embedded in SiO₂ have been

determined with spectroscopic ellipsometry (SE), and the influence of thermal annealing on the dielectric functions has also been investigated.

30 nm SiO₂ thin films were thermally grown in dry oxygen at 950 °C on a *p*-type Si (100) wafer. Si ions with a dose of 8×10^{16} cm⁻² were then implanted into the SiO₂ thin films at 1 keV. Postimplantation thermal annealing was carried out in N₂ at various annealing temperatures for different durations. The mean size of nc-Si was estimated from full width at half maximum (FWHM) of the Bragg in the x-ray diffraction (XRD) measurement.^{3,4} The average size of nanocrystals was estimated to be ~ 3 – 4 nm. It was found that the nc-Si size changes little with annealing. This observation is consistent with those reported in literatures.^{6,15} The cross-sectional transmission electron microscopy (TEM) measurement reveals the existence of a densely stacked Si nanocrystal layer with a thickness of ~ 16 nm embedded in SiO₂, as shown in Fig. 1. The sample is annealed at 1000 °C for 20 min (i.e., sample a). To determine the optical properties of the densely stacked Si nanocrystal layer, SE measurements were carried out in the wavelength range of 250–1100 nm with a step of 5 nm, and the incident angle was set at 75°.

For the SE analysis, an appropriate optical model is required. As a densely stacked Si nanocrystal layer is formed in the SiO₂ thin film, the model developed for the isolated nc-Si embedded in a SiO₂ matrix^{3,4} is inadequate for the present study. In the present study, a single layer of densely stacked nc-Si is embedded in the SiO₂ thin film as revealed by the TEM image shown in Fig. 1 and the situation is different from that of the isolated nc-Si dispersedly distributed in a SiO₂ matrix.^{3,4} Obviously, this densely stacked nc-Si layer should be treated as a phase in the ellipsometric analysis. Therefore, a five-phase model, namely, air/SiO₂ layer/

^{a)}Electronic mail: ding0008@ntu.edu.sg

^{b)}Electronic mail: echentp@ntu.edu.sg

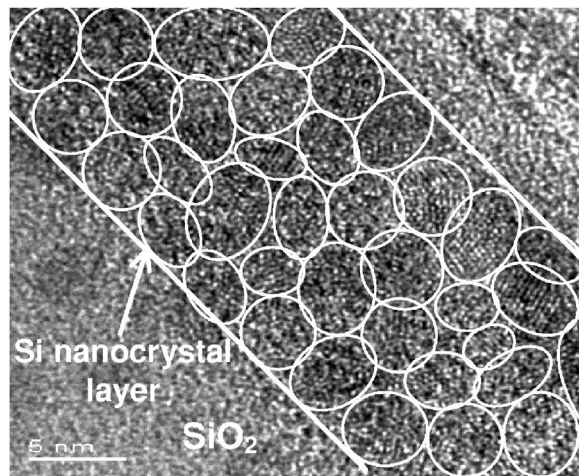


FIG. 1. Cross-sectional TEM image of the densely stacked Si nanocrystal layer embedded in SiO_2 thin film for sample a.

densely stacked nc-Si layer/ SiO_2 layer/Si substrate, which is shown in Fig. 2(a), was employed to carry out the SE fittings in the present study. Note that in this model, the ellipsometric angles (Ψ and Δ) are functions of the thicknesses and dielectric functions of all the layers. Excellent fittings with meaningful outputs have been achieved with this model. Note that no optical dispersion model was required for the SE fittings with the model. As an example, Fig. 2(b) shows the spectral fitting of Ψ and Δ for sample a (i.e., the sample annealed at 1000°C for 20 min). As can be seen in this figure, all the complicated spectral features of both Ψ and Δ can be fitted excellently, indicating that the model shown in Fig. 2(a) is effective.

Figure 3 shows the dielectric functions of the densely stacked silicon nanocrystal layer for sample a. For comparison,

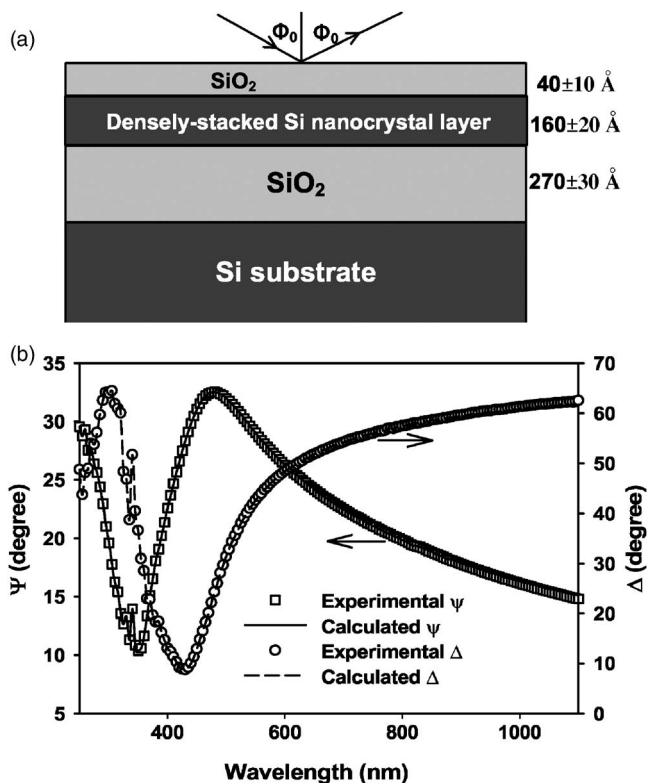


FIG. 2. (a) Five-phase model used in the SE analysis. (b) Spectral fittings of Ψ and Δ for sample a.

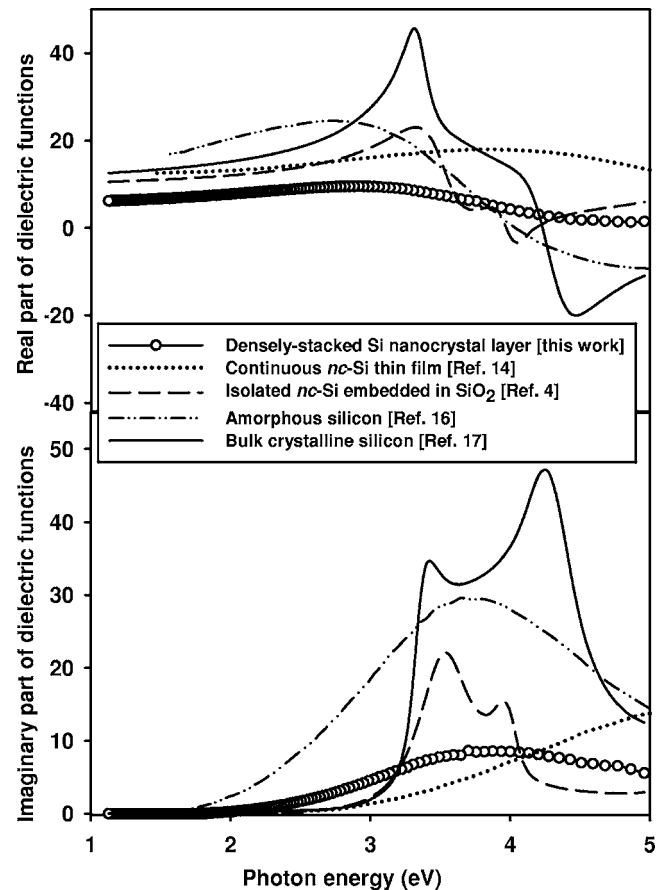


FIG. 3. Real (ϵ_1) and imaginary (ϵ_2) parts of the complex dielectric functions of the densely stacked Si nanocrystal layer for sample a. For comparison, the dielectric functions of the continuous nc-Si thin film (Ref. 14), the isolated nc-Si dispersedly distributed in a SiO_2 matrix (Ref. 4), amorphous Si (Ref. 16), and bulk crystalline Si (Ref. 17) are also included in this figure.

son, the dielectric functions of other Si materials are also included in Fig. 3. As can be seen in the figure, the dielectric spectra of the densely stacked silicon nanocrystal layer are similar to that of amorphous Si but different from those of both bulk crystalline Si and the isolated nc-Si. For the imaginary part of dielectric functions, the densely stacked silicon nanocrystal layer and amorphous Si show a single broadened peak; in contrast, bulk crystalline Si and the isolated nc-Si exhibit a two-peak structure. The peak structures in the dielectric spectra are believed to originate from singularities in the joint density of states (DOS). Essentially, the DOS in the amorphous state is a broadened version of crystalline state, which leads to a single broad peak in the dielectric spectra of amorphous semiconductors. Therefore, the single peak structure may suggest that the nanocrystal layer is in an amorphous state to a certain extent. On the other hand, the nanocrystal layer also shows significant reductions in the amplitude of dielectric functions as compared with bulk crystalline Si and amorphous Si, which is related to the size effect of the nanocrystals.^{3,4}

Furthermore, we observed a significant influence of the annealing on the dielectric functions of the densely stacked Si nanocrystal layer. Figure 4 shows the imaginary part of dielectric functions of the densely stacked silicon nanocrystal layer synthesized at a fixed annealing temperature of 1000°C for different annealing durations. The dielectric function changes with the annealing duration, showing a trend towards bulk crystalline Si. Firstly, the dielectric func-

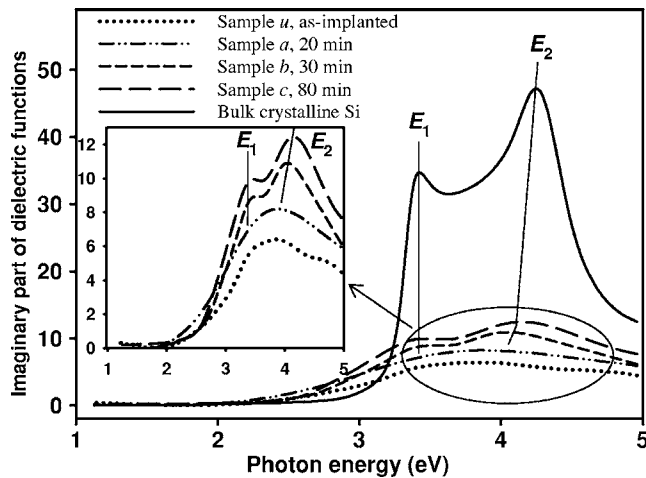


FIG. 4. Influence of annealing duration on the imaginary (ϵ_2) part of the complex dielectric functions of the densely stacked Si nanocrystal layer. The annealing temperature is fixed at 1000 °C.

tion increases with the annealing duration. Secondly, the dielectric function exhibits a clear two-peak structure when the annealing duration is 30 min, and the structure is further enhanced when the annealing duration is 80 min. The structure is analogous to that of bulk Si which has two peaks at the transition energies E_1 (~3.4 eV) and E_2 (~4.3 eV) as its critical points. E_1 of the nanocrystal layer is about the same as that of bulk crystalline Si, and it changes very little with the annealing duration. However, E_2 of the nanocrystal layer is slightly lower than that of bulk Si, but it shows a small blueshift towards that of bulk Si with the increase in annealing duration. However, it should be pointed out that extending the annealing duration should not result a dielectric function that is approaching that of bulk crystalline Si because of the quantum size effect of the nc-Si and the difference in the structure between the two materials. A similar annealing effect on the dielectric functions is also observed from the experiment of various annealing temperatures. Figure 5 shows the evolution of the dielectric functions with annealing temperature for the fixed annealing duration of 20 min. One can observe from Fig. 5 together with Fig. 3 that for the

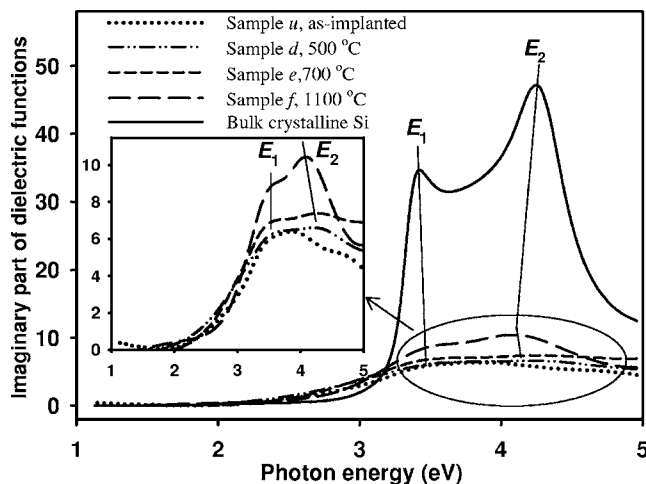


FIG. 5. Influence of annealing temperature on ϵ_2 of the densely stacked Si nanocrystal layer. The annealing duration is 20 min.

annealing duration of 20 min, only a single broad peak in the dielectric spectra exists when the annealing temperature is 1000 °C or lower, but a two-peak structure emerges when the annealing temperature is 1100 °C. Therefore, it is clear that thermal annealing promotes the evolution of the dielectric functions towards that of bulk crystalline Si. The mechanism for the annealing effect is not known yet, but one may attribute it to the crystallization and or the growth of the nanocrystals caused by the annealing.

In summary, the dielectric functions of the densely stacked Si nanocrystal layer embedded in SiO₂ have been determined with spectroscopic ellipsometry. It is observed that thermal annealing has a strong influence on the dielectric functions. For the fixed annealing temperature of 1000 °C, if the annealing duration is 20 min or shorter, the dielectric functions are similar to that of amorphous Si, showing a single broad peak in the dielectric spectra; however, a two-peak structure, which is analogous to that of bulk crystalline Si, emerges when the annealing duration is 30 min or longer. For the fixed annealing duration of 20 min, if the annealing temperature is 1000 °C or lower, the dielectric functions are similar to that of amorphous Si, but the two-peak structure emerges when the annealing temperature is 1100 °C. In conclusion, thermal annealing promotes the evolution of the dielectric functions from the amorphous state towards crystalline state.

This work has been financially supported by the Ministry of Education, Singapore, under Project No. ARC 1/04.

- ¹P. Mutti, G. Ghisloti, S. Bertoni, L. Bonoldi, G. F. Cerofolini, L. Meda, E. Grill, and M. Guzzi, *Appl. Phys. Lett.* **66**, 851 (1995).
- ²Y. Q. Wang, R. Smirani, and G. G. Ross, *Nano Lett.* **4**, 2041 (2004).
- ³T. P. Chen, Y. Liu, M. S. Tse, O. K. Tan, P. F. Ho, K. Y. Liu, D. Gui, and A. L. K. Tan, *Phys. Rev. B* **68**, 153301 (2003).
- ⁴L. Ding, T. P. Chen, Y. Liu, C. Y. Ng, and S. Fung, *Phys. Rev. B* **72**, 125419 (2005).
- ⁵S. Guha, S. B. Qadri, R. G. Musket, M. A. Wall, and Tsutomu Shimizu-Iwayama, *J. Appl. Phys.* **88**, 3954 (2000).
- ⁶M. Carrada, N. Cherkashin, C. Bonafos, G. Benassayag, D. Chassaing, P. Normand, D. Tsoukalas, V. Soncini, and A. Claverie, *Mater. Sci. Eng., B* **101**, 204 (2003).
- ⁷P. Normand, K. Beltsios, E. Kapetanakis, D. Tsoukalas, T. Travlos, J. Stoemenos, J. Van Den Berg, S. Zhang, C. Vieu, H. Launois, J. Gautier, F. Jourdan, and L. Palun, *Nucl. Instrum. Methods Phys. Res. B* **178**, 74 (2001).
- ⁸C. Bonafos, M. Carrada, N. Cherkashin, H. Coffin, D. Chassaing, G. Benassayag, A. Claverie, T. Müller, K. H. Heinig, M. Perego, M. Fanciulli, P. Dimitrakakis, and P. Normand, *J. Appl. Phys.* **95**, 5696 (2004).
- ⁹C. Y. Ng, T. P. Chen, L. Ding, and S. Fung, *IEEE Electron Device Lett.* **27**, 231 (2006).
- ¹⁰K. Luterova, I. Pelant, J. Valenta, J.-L. Rehspringer, D. Muller, J. J. Grob, J. Dian, and B. Honerlage, *Appl. Phys. Lett.* **77**, 2952 (2000).
- ¹¹L. Pavesi, L. Dal Negro, C. Mazzoleni, F. Franzo, and F. Priolo, *Nature (London)* **408**, 440 (2000).
- ¹²H.-Ch. Weissker, J. Furthmüller, and F. Bechstedt, *Phys. Rev. B* **65**, 155327 (2002).
- ¹³H.-Ch. Weissker, J. Furthmüller, and F. Bechstedt, *Phys. Rev. B* **67**, 165322 (2003).
- ¹⁴D. Amans, S. Callard, A. Ganaire, J. Joseph, G. Ledoux, and F. Huisken, *J. Appl. Phys.* **93**, 4173 (2003).
- ¹⁵M. Lopez, B. Garrido, C. Bonafos, A. Perez-Rodriguez, and J. R. Morante, *Solid-State Electron.* **45**, 1495 (2000).
- ¹⁶D. E. Aspnes, A. A. Studna, and E. Kinsbron, *Phys. Rev. B* **29**, 768 (1984).
- ¹⁷D. E. Aspnes and A. A. Studna, *Phys. Rev. B* **27**, 985 (1983).